

Grid Compliance and Performance Analysis of a Hybrid Load–Generation Site Integrating Wind Farm, Battery Storage, and Hydrogen Generation

Mohamed Abouyehia¹, Anup Nambiar², Irfan Yousuf², Michael Smailes², Khaled H. Ahmed¹

¹*Department of Electronic and Electrical Engineering, University of Strathclyde, Glasgow, G1 1XQ, UK*

²*Offshore Renewable Energy Catapult Glasgow, UK*

mohamed.abouyehia@strath.ac.uk, anup.nambiar@ore.catapult.org.uk, irfan.yousuf@ore.catapult.org.uk,
michael.smailes@ore.catapult.org.uk, khaled.ahmed@strath.ac.uk

Abstract—The increasing penetration of hybrid load–generation sites is expected to play a pivotal role in future power grids. This paper investigates the challenges associated with a hybrid load–generation site comprising offshore wind farms (OWFs), battery energy storage systems (BESS), and hydrogen production units, with a focus on its impact on grid compliance. The study begins with a detailed numerical modelling of the entire hybrid site in PSCAD, incorporating real-world technologies such as Siemens-Gamesa wind turbines, ABB eStorage Max-STPP BESS and Siemens Silyzer 300 electrolyser systems to ensure accurate representation of industrially deployed components. The proposed hybrid site includes a 1.2 GW OWF, a 400 MW BESS, and a 400 MW electrolyser plant, all operating behind a single 400 kV grid connection point. Scenario-based simulations reveal several critical challenges associated with the operation of hybrid load–generation sites. These include the slow dynamics of electrolysers, high reactive power requirements from transmission infrastructure, and constraints in fault ride-through performance. To address these issues, potential mitigation solutions are thoroughly analysed and evaluated. The findings, verified through PSCAD simulations, provide a comprehensive understanding of regulatory compliance in large-scale hybrid energy systems and present practical recommendations for the development of future grids.

Keywords—Hybrid load-generation sites, grid compliance, large scale renewable integration, hydrogen production.

I. INTRODUCTION

The transition toward renewable energy sources such as wind and solar is fundamentally reshaping modern power networks [1]. As grids transition toward low-carbon solutions, hybrid load-generation sites have emerged as a key strategy for enhancing flexibility and managing supply-demand variability. These sites integrate multiple energy assets, including OWFs, BESS, and hydrogen electrolysis units. By combining short-term storage technologies such as batteries with long-term hydrogen storage, hybrid systems can reduce curtailment. For instance, the Hornsea three OWF in the United Kingdom, with an installed capacity of 2.9 GW, is investigating battery storage solutions to manage short-term power fluctuations [2]. Similarly, the 1.5-gigawatt Hollandse Kust Zuid offshore wind project in the Netherlands is

exploring the integration of electrolysis-based hydrogen production for long-term energy storage [3]. As the scale and complexity of such sites continue to grow, advanced modelling and control methodologies are required to ensure stable operation and ensure compliance with grid codes.

The existing literature on hybrid load-generation sites can be broadly classified into three primary areas: planning and techno-economic analysis, system design and optimisation, and control strategies aimed at ensuring grid compliance and operational stability. Regarding planning and techno-economic analysis, several studies have explored the feasibility and cost-effectiveness of hybrid sites. For instance, the authors in [3] demonstrated the financial and environmental benefits of integrating hydrogen storage, but it did not address large-scale grid compliance. Similarly, the authors in [4] examined the economic and operational feasibility of hybrid sites, with an emphasis on optimising system costs rather than addressing grid stability considerations. On the other hand, the authors in [5] provided a broader review of hybrid system planning, though their focus was primarily on small-scale implementations. In terms of site design and optimisation, the authors in [6] investigated a standalone hybrid site and analysed its performance under varying wind conditions. The author in [7] explored hybrid on-grid sites with multiple DC-DC converters for energy dispatch and validated their effectiveness in maintaining stability but limiting the analysis to low-voltage applications. From another perspective, control strategies for grid compliance remain a critical challenge, particularly in ensuring low-voltage ride-through (LVRT) and ancillary services. For instance, the author in [8] implemented a control method for DC bus voltage regulation and MPPT in wind and PV sources. However, this control method lacked advanced grid support features. The authors in [9] introduced a dynamic feed-forward LVRT control scheme for a grid-connected hybrid energy system. Their approach utilised negative sequence current minimisation to improve grid stability, particularly during voltage sags.

Despite significant advancements in hybrid site integration, there is a lack of comprehensive studies that combine offshore wind, battery energy storage, and hydrogen-based fuel

This research was funded through the joint industry Integrator programme hosted by the Carbon Trust. The industrial partners in this programme are EnBW, ScottishPower, SSE Renewables, Vattenfall, TotalEnergies, and Shell.

generation into a unified large-scale hybrid load-generation site, while simultaneously evaluating compliance with grid codes. Existing research predominantly focuses on economic feasibility, planning, and small-scale implementations, with limited investigations into large-scale grid compliance. Most studies also emphasise low-voltage applications, leaving a significant gap in understanding high-voltage grid integration and the associated challenges of regulatory compliance.

To address these gaps, this paper presents a comprehensive numerical modelling and performance analysis of a large-scale hybrid load–generation site comprising a 1.2 GW OWF, a 400 MW BESS, and a 400 MW electrolyser plant. Real-world technologies, including Siemens-Gamesa wind turbines, ABB eStorage Max-STPP BESS, and Siemens Silyzer 300 electrolyser systems, are incorporated into the model to ensure industrial relevance and accuracy. The study focuses on assessing the grid compliance of the hybrid site, including fault ride-through capabilities, voltage regulation, and the provision of ancillary services to enhance grid stability. Through scenario-based PSCAD simulations, the research identifies critical challenges associated with the grid integration of large-scale hybrid sites and proposes potential solutions to effectively address these issues.

The organisation of the paper is as follows: Section II details the modelling of the OWFs, BESS, and hydrogen production units. Section III investigates the dynamic performance of the hybrid site through PSCAD simulations. Section IV concludes with a summary of the main findings and suggests directions to facilitate high-power hybrid sites in future grids.

II. MODELLING OF THE HYBRID LOAD–GENERATION SITE

This section presents the development of the numerical models of the OWF, BESS, and electrolyser plant in PSCAD. These models are designed to accurately represent the electrical, mechanical, and dynamic characteristics of the hybrid site. Moreover, each model is constructed with detailed control strategies, including converter control, reactive power management, and fault ride-through capabilities. The following subsections detail the modelling of each component.

A. Generic OWF PSCAD Model

This section presents the numerical modelling of the OWF in PSCAD, including the wind turbines, collector system, offshore and onshore substations, transmission system, and reactive power compensation strategy.

1) Wind Turbine Model

Each wind turbine in the model is based on the Siemens-Gamesa SG 10.0-193 DD, a 10 MW direct-drive turbine with a permanent magnet synchronous generator (PMSG) [10, 11]. The generator produces a variable-frequency AC output of 690 V at 13 Hz. The turbine is connected to a full-scale back-to-back power converter, which consists of a machine-side converter (MSC) and a grid-side converter (GSC), linked through a DC-link capacitor. The MSC regulates the generator speed and controls the active power extracted from the wind.

The GSC converts the DC-link power back into AC at 690 V and 50 Hz, ensuring synchronisation with the grid. The GSC is responsible for DC-link voltage regulation and reactive power support. The DC-link voltage is controlled at a nominal voltage of 1.5 kV. The turbine output voltage is stepped up from 690 V to 66 kV using a three-phase, two-winding transformer to connect it to the collector system.

2) Collector System Model

The collector system aggregates power from individual turbines and transmits it to the offshore substation. The wind farm consists of 30 feeders, as shown in Fig. 1, each collecting power from four turbines, with a total of three collector systems, each rated at 400 MW. The three collector systems have 10 feeders each. In Fig. 1, collector system 1 (blue) has feeder lengths of 13.5 km, collector system 2 (red) has feeder lengths of 7.5 km, and collector system 3 (green) has feeder lengths of 10.5 km. The varying separation distances between turbines are influenced by factors such as the physical layout of the terrain, which may include hills, valleys, or obstructions, and the need to minimize wake effects. This variation adds realism to the model [12]. The feeders are designed for 66 kV operation and are modelled in PSCAD using PI-section cable models. The equivalent impedance of each collector system is modelled based on its length to ensure an accurate representation of the voltage drops across the collector network.

3) Onshore and Offshore Substations

The offshore substation steps up the voltage from 66 kV to 220 kV for efficient power transmission to shore. It consists of three 450 MVA transformers in a delta-star configuration,

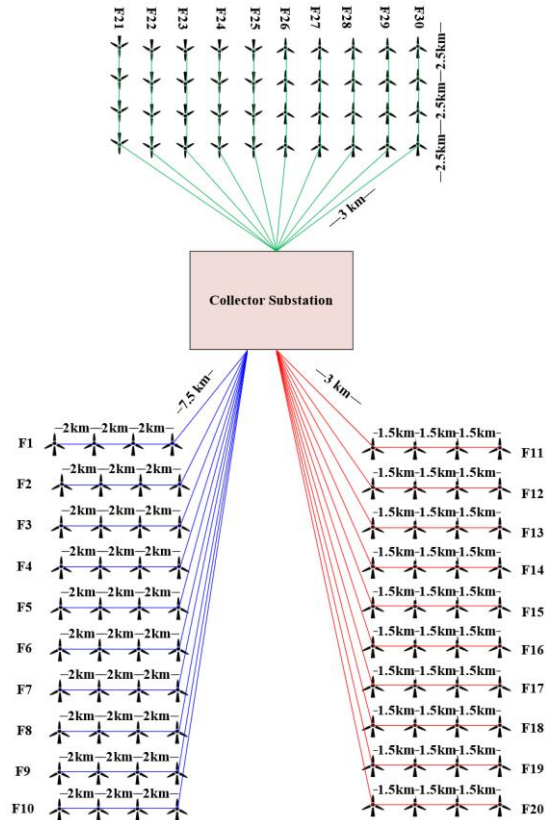


Fig. 1 Collector system.

each rated for 220/66 kV operation. The onshore substation on the other hand steps up the voltage from 220 kV to 400 kV for integration into the national grid. It consists of three 450 MVA transformers in a star-star configuration to ensure compatibility with the high-voltage transmission system.

4) AC Transmission System Model

The OWF transmits power to shore through three submarine cables, each being a three-core design with 1600 mm² copper conductors, operating at 220 kV and rated for 450 MVA per cable. The transmission distance is 80 km; therefore, a frequency-dependent model is used in PSCAD to accurately capture the electrical characteristics of the cables, as frequency-dependent effects become more significant over long distances.

5) Reactive Power Compensation Strategy

The OWF requires reactive power compensation to counteract the effects of the submarine transmission cables and collector system, which generate excessive capacitive reactive power. To ensure grid code compliance and maintain unity power factor at the grid point of coupling, compensation is provided through a combination of shunt reactors and STATCOM. Three shunt reactors, each rated at 160 MVAR, are installed at the offshore substation, positioned before the transmission cables to compensate for the reactive power generated by the 66 kV collector system and submarine cables. Additionally, three shunt reactors, each rated at 100 MVAR, are installed at the onshore substation, positioned after the transmission cables to further compensate for the excess reactive power before grid integration. These six shunt reactors collectively compensate for approximately 80% of the reactive power generated by the transmission and collection network. The remaining 20% of the required reactive power compensation is provided by a STATCOM installed at the onshore substation, ensuring unity power factor operation at the 400 kV grid connection point. Fig. 2 shows the PSCAD model of the generic OWF.

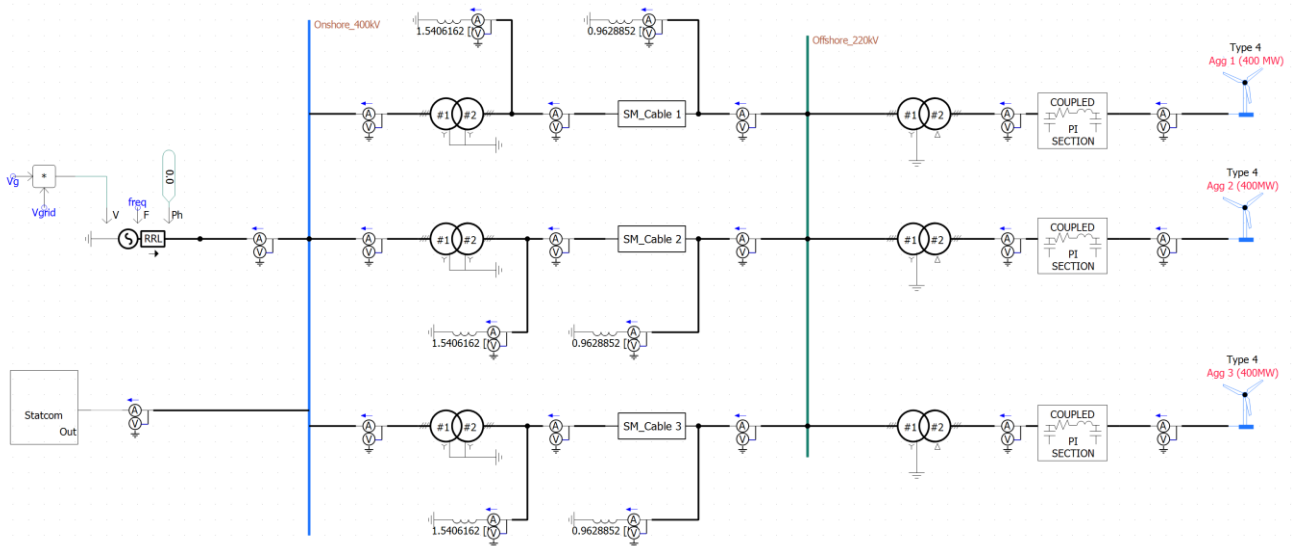


Fig. 2 Generic OWF PSCAD Model.

B. Generic BESS PSCAD Model

This part presents the numerical modelling of the BESS in PSCAD. It covers the battery modules and their power conversion system.

1) Battery Module Model

The characteristics of the commercial ABB eStorage Max-STPP system are used to model the battery modules in PSCAD [13]. The PSCAD BESS model consists of 200 lithium iron phosphate (LFP) battery modules, each rated at 2 MW, resulting in a total power capacity of 400 MW and an energy storage capacity of 550 MWh. Each module operates at a nominal DC voltage of 1.5 kV and is modelled using Shepherd method [14].

2) Power Conversion System

The power conversion system for the battery consists of bi-directional inverters, each rated at 2.5 MW, converting DC power from the battery modules into AC power at 690 V for grid integration. These inverters operate in grid-following mode. Under normal operating conditions, the reactive power setpoint is maintained at zero, and the battery system is controlled to either charge or discharge at a specified active power level based on grid demand. However, during grid faults, the control priority shifts, giving reactive power support higher priority. In such scenarios, the BESS inverters actively inject reactive power to support grid voltage recovery, to ensure compliance with fault ride-through requirements.

3) Grid Integration

Each pair of battery modules is connected to a three-phase, three-winding distribution transformer rated at 5 MVA, stepping up the voltage from 690 V to 13.8 kV. A total of 100 distribution transformers are deployed, each dedicated to every pair of the battery modules. The aggregated battery output is then stepped up to 400 kV through a main transformer rated at 450 MVA to integrate with the transmission grid. Fig. 3 shows the PSCAD model of the generic BESS.

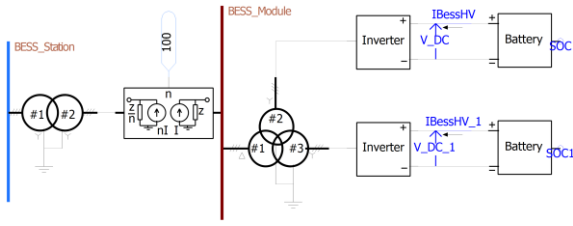


Fig. 3 Generic BESS PSCAD Model.

C. Generic Electrolyser Plant PSCAD Model

This section presents the numerical modelling of the electrolyser plant in PSCAD, covering the electrolysis process, power conversion system, and compression system.

1) Electrolyser Module Model

The electrolyser plant consists of 23 Siemens Silyzer 300 PEM electrolyser modules, each rated at 17.5 MW, resulting in a total capacity of 400 MW. Each PEM electrolyser offers start-up and shut-down times (between 1 second and 5 minutes) and a ramp rate (up to 10% per second) [15]. Each electrolyser module operates at a nominal DC voltage of 1.2 kV and has a hydrogen production capacity reaching up to 335 kg/h. The minimum load for a single module is 20%. In PSCAD, the Silyzer 300 module is modelled as a current dependent voltage source, with its hydrogen production rate determined by Faraday’s law of electrolysis. The model accounts for voltage, resistance, and temperature, based on the U-I characteristic equation of the electrolytic cell [16].

2) Power Conversion System and Harmonic Filtering

To convert AC grid power into the required DC voltage for the electrolyzers, the system employs a 12-pulse thyristor rectifier. The 12-pulse configuration is selected to reduce harmonic distortion, thereby improving power quality at the PCC. Each rectifier is rated at 20 MVA. As the 12-pulse rectifier system generates harmonics of the order $12n \pm 1$, additional harmonic mitigation is necessary to comply with grid power quality standards.

3) Grid Integration

Each thyristor rectifier, along with its associated electrolyser module, connects to the main transformer through a three-phase, three-winding distribution transformer, configured in a Y-Y- Δ arrangement. These transformers step up the voltage from 1 kV on the electrolyser side to 13.8 kV on the grid side. Each distribution transformer is rated at 20 MVA. A total of 23 distribution transformers are deployed, each dedicated to one electrolyser module and its respective rectifier unit. The main transformer is a three-phase transformer, stepping up the voltage from 13.8 kV to 400 kV for grid integration. It is rated at 500 MVA.

4) Hydrogen Compression and Balance of Plant

The 400 MW hydrogen production plant generates a hydrogen mass flow rate of 0.093 kg/s. The hydrogen output, initially at 1.1 bar, undergoes multi-stage compression using centrifugal compressors to reach the commercial pressure requirement of 80 bar. The total power required for compression is approximately 5 MW. The motors for the compressors are connected to the main bus via a three-phase,

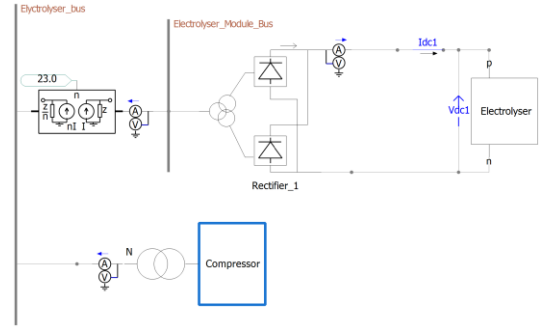


Fig. 4 Generic Electrolyser PSCAD Model.

two-winding transformer with a voltage ratio of 13.8 kV/6.6 kV and a nominal power rating of around 5 MVA. Fig. 4 shows the PSCAD model of the generic electrolyser.

III. RESULTS AND DISCUSSION

This section presents the results of the numerical simulations and validates the performance of the hybrid load generation system under multiple scenarios. The objective is to illustrate the challenges associated with integrating OWFs, BESS, and electrolyser plants behind a single grid connection point and to assess their impact on the power system. The scenarios investigate different aspects of system operation, including reactive power requirements, dynamic response characteristics, and fault ride-through capability. For all scenarios, the measurements for the STATCOM, grid, and wind farm are conducted at the high-voltage 400 kV onshore bus. For the BESS and electrolyser, the measurements are taken at the low-voltage side, prior to their main transformer.

A. Scenario 1: Reactive Power Challenge Without Compensation

The first scenario evaluates the activation of the hybrid system without reactive power compensation. This scenario examines the reactive power demand of the submarine cables and twelve-pulse rectifiers, highlighting the potential challenges for the grid in the absence of reactive power compensation. In

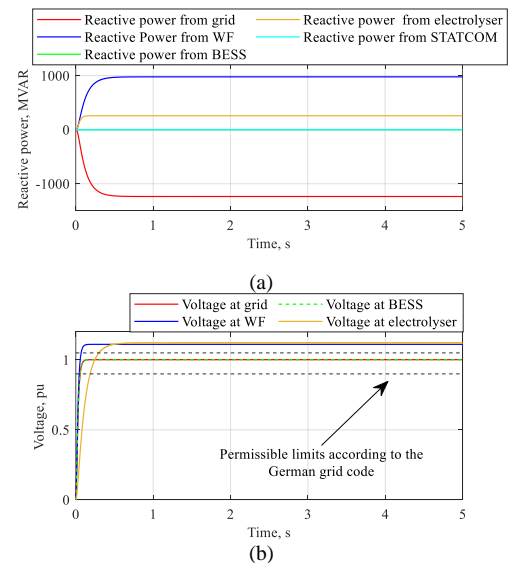


Fig. 5 Results of Scenario 1: (a) Reactive power exchange at different buses, and (b) voltage response at key buses.

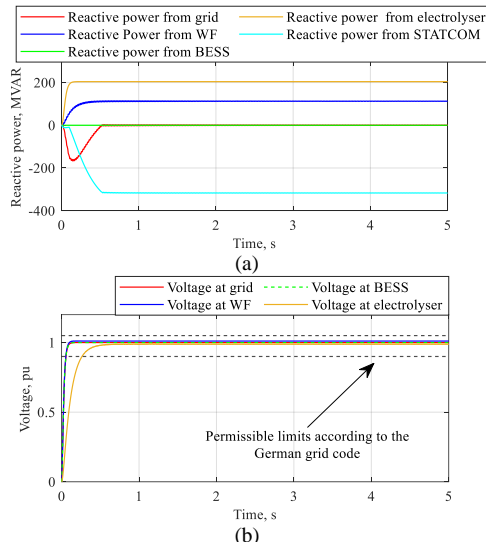


Fig. 6 Results of scenario 1 but with reactive power compensation system: (a) reactive power at different buses, and (b) voltage response at key buses.

this scenario, the wind farm remains disabled, and both the BESS and electrolyser are in idle mode to isolate and examine the reactive power flow through the grid. Fig. 5 shows the results for this scenario. Fig. 5(a) illustrates the significant reactive power demand introduced by the system components. The submarine cables alone contribute approximately 975 MVAR at no load due to their inherent capacitance, while the twelve-pulse rectifiers introduce an additional 260 MVAR due to the low firing angle in idle mode. This results in a total reactive power demand of approximately 1235 MVAR, which is a significant amount for the grid to supply. Consequently, the voltage at the offshore substation and the electrolyser bus exceeds the permissible limits stipulated by the German grid code, as shown in Fig. 5(b), highlighting the necessity of a reactive power compensation system to ensure grid compliance. To mitigate this issue, a compensation system consisting of six shunt reactors (three before and three after the submarine cable) and onshore STATCOM are introduced. Fig. 6 shows the results for scenario 1 but with the compensation system. As shown in Fig. 6(a), the reactive power demand of the OWF is significantly reduced to approximately 111 MVAR, which is further compensated by an onshore STATCOM. The STATCOM supplies the remaining reactive power required by the submarine cables and the electrolyser converter, thereby achieving unity power factor at the grid connection point. The initial dip in the grid reactive power (red curve) is due to the grid supporting reactive power until the STATCOM starts up. Additionally, Fig. 6(b) confirms that the voltage levels at all buses remain

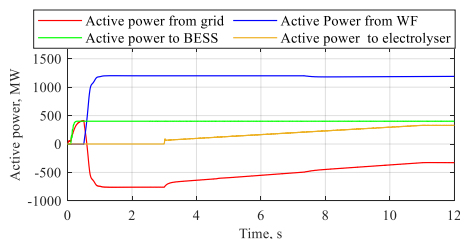


Fig. 7 Active power distribution across the hybrid system for scenario 2.

within the permissible limits defined by the grid code. The secondary winding of the main transformer supplying the electrolyser plant should be equipped with an automatic tap changer. Due to the high reactive power of the twelve-pulse rectifier at no-load, the voltage can exceed permissible limits. To address this, the tap changer is set to -10% under no-load conditions to ensure voltage remains within acceptable levels.

B. Scenario 2: Dynamic Response of the Hybrid System Component

The second scenario investigates the slow dynamic response of the electrolyser relative to the fast dynamics of the BESS and OWF. Electrolysers exhibit slow response due to their inherent ramping limitations, typically 10% of their capacity per second, whereas the BESS and wind farm can respond almost instantaneously to power changes. Fig. 7 shows the results of scenario 2. As shown in Fig. 7, at $t = 0.1$ s, the BESS is charged from the grid at full power, transitioning from idle mode to full charging within milliseconds. At $t = 0.5$ s, the wind farm is activated and ramps up to its full capacity of 1.2 GW within 0.5 seconds, demonstrating its fast response capability. As the wind farm reaches full power, the energy used to charge the BESS is supplied from the wind farm instead of the grid, and the remaining surplus power is transmitted to the grid. At $t = 3$ s, the electrolyser is activated. Unlike the BESS, the electrolyser does not immediately consume power but instead requires a minimum power threshold of 20% of its capacity to begin operation. This minimum power requirement introduces an operational constraint, as any power below this threshold is insufficient for the electrolyser to function. Once the minimum power is reached, the electrolyser gradually ramps up, requiring approximately 8 seconds to reach full capacity. This slow ramping characteristic presents a challenge for the power system. One of the hybrid system components—either the grid, BESS, or wind farm—must coordinate its power output to align with the electrolyser slow response dynamics, ensuring a balance between generation and load. Additionally, another critical issue observed in this scenario is the relatively low efficiency of the electrolyser. Despite the wind producing 1.2 GW, system losses amount to 146 MW, corresponding to 12% of total generation, with the majority being heat dissipation within the electrolyser due to its low efficiency of 75%. This underscores the need for optimal power dispatch strategies to maximise the economic efficiency of the hybrid system, ensuring that available wind energy is utilised effectively between the grid, BESS and electrolyser.

C. Scenario 3: Fault Ride-Through Capability of the Hybrid System

The third scenario investigates the fault ride-through capability of the hybrid system. It assesses how the BESS, wind farm, and electrolyser respond to a grid fault and low voltage scenarios. As shown in Fig. 8(a), a fault occurs at $t = 12$ s, causing the grid bus voltage to drop to 0.1 p.u. Similar voltage drops are observed across other system buses, albeit with varying severity. In response, both the BESS and wind farm immediately reduce their active power, as shown in Fig. 8(b). Moreover, The electrolyser active power drops to zero. The BESS increases its reactive power output to 125 MVAR,

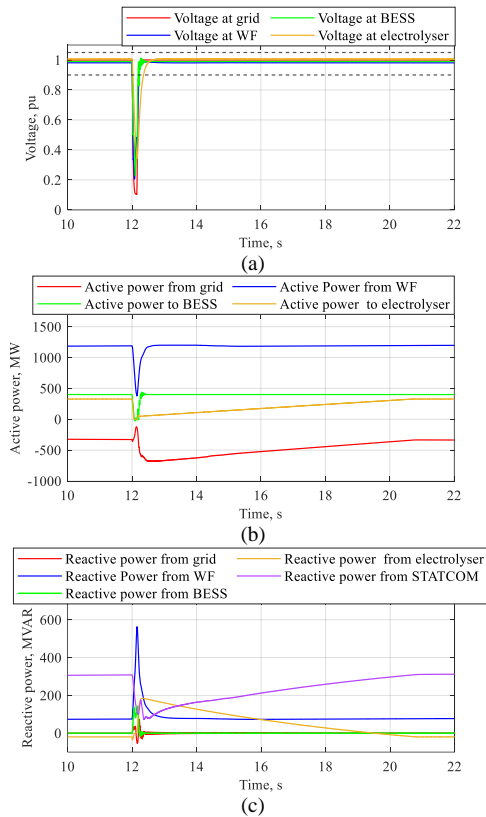


Fig. 8 Results of Scenario 3: (a) Voltage response at key buses, (b) active power across the hybrid system, and (c) reactive power at different buses.

while the wind farm also prioritises reactive power injection to support voltage recovery, as shown in Fig. 8(c). Moreover, the STATCOM is expected to provide its rated reactive power (400 MVAR). However, as the nearest component to the fault, it experiences a low voltage of approximately 0.1 pu. Delivering full reactive power at this voltage would require exceeding the 1.2 pu current limit set to protect the power electronic switches. As the current saturates at this limit, the low voltage results in reduced reactive power output. Following fault clearance, the system faces a post-fault recovery challenge due to the slow ramping of the electrolyser. As previously observed, the electrolyser ramps up at 10% of its capacity per second, meaning that full recovery takes several seconds. During this period, the grid should compensate for the gradual increase in electrolyser load, adjusting power dispatch accordingly. If the grid lacks sufficient flexibility, the wind farm must dynamically regulate their output to maintain system load-generation balance. Another critical aspect observed in this scenario is the reactive power variation of the electrolyser. The twelve-pulse rectifier consumes the highest reactive power at no load, due to its low firing angle, but as the electrolyser ramps up, its reactive power demand decreases sharply. Without a dedicated STATCOM, this variation would impose a fluctuating reactive power burden on the grid. The presence of a STATCOM enhances system flexibility, ensuring that reactive power variations are managed locally.

IV. CONCLUSION

This paper presented the modelling and performance analysis of a large hybrid load-generation site, comprising a 1.2 MW OWF, a 400 MW BESS, and a 400 MW electrolyser plant. It addressed key grid compliance challenges. The study highlighted the main issues including the significant reactive power demand from submarine cables and twelve-pulse rectifiers, requiring combined compensation through shunt reactors and STATCOM. Additionally, the mismatch in dynamic response, with the electrolyser's slow ramping compared to the fast response of the OWF and BESS, emphasised the need for coordinated control strategies to ensure load-generation balance. Furthermore, the fault ride-through analysis revealed the importance of advanced reactive power support during faults and the challenge of electrolyser recovery post-fault. These findings contribute to understanding and resolving the critical challenges of integrating large-scale hybrid sites into future power grids.

REFERENCES

- [1] Q. Hassan *et al.*, "The renewable energy role in the global energy Transformations," *Renewable Energy Focus*, vol. 48, p. 100545, 2024.
- [2] Ørsted, "BESS co-located with Hornsea 3 Offshore Wind Farm." Ørsted <https://hornseaproject3.co.uk/news/2024/06/orsted-invests-in-battery-energy-storage-system-co-located-with-hornsea-3> (accessed 2025).
- [3] M. Hunik, "A techno-economic approach to optimizing off-grid offshore wind-based hydrogen production," 2024.
- [4] V. M. Fontalvo, G. J. Nelson, O. Pupo-Roncillo, M. E. Sanjuan, and H. A. Gómez, "A techno-economic assessment for fuel cells hybrid systems in stationary applications," *International Journal of Sustainable Energy*, vol. 42, no. 1, pp. 889-912, 2023.
- [5] K. S. Krishna and K. S. Kumar, "A review on hybrid renewable energy systems," *Renewable and Sustainable Energy Reviews*, vol. 52, pp. 907-916, 2015.
- [6] K. R. Jyothy, C. P. Raju, and R. Srinivasarao, "Simulation studies on WTG-FC-battery hybrid energy system," in *2017 International Conference on Innovative Mechanisms for Industry Applications (ICIMIA)*, 2017: IEEE, pp. 710-716.
- [7] N. A. Ahmed, "On-grid hybrid wind/photovoltaic/fuel cell energy system," in *2012 10th International Power & Energy Conference (IPEC)*, 2012: IEEE, pp. 104-109.
- [8] N. A. Ahmed, A. Al-Othman, and M. AlRashidi, "Development of an efficient utility interactive combined wind/photovoltaic/fuel cell power system with MPPT and DC bus voltage regulation," *Electric Power Systems Research*, vol. 81, no. 5, pp. 1096-1106, 2011.
- [9] A. K. Roy, G. R. Biswal, and P. Basak, "An integrated rule-based power management and dynamic feed-forward low voltage ride through scheme for a grid-connected hybrid energy system," *Journal of Renewable and Sustainable Energy*, vol. 12, no. 5, 2020.
- [10] A. Bensalah, G. Barakat, and Y. Amara, "Electrical generators for large wind turbine: Trends and challenges," *Energies*, 2022.
- [11] Siemens-Gamesa https://www.thewindpower.net/turbine_en_1662_siemens-gamesa_sg-10.0-193-dd.php (accessed 2025).
- [12] J. Roy, H. Liu, I. Ndiaye, and R. Datta, "DC collection and transmission for offshore wind farms," in *2023 IEEE Energy Conversion Congress and Exposition (ECCE)*, 2023: IEEE, pp. 337-343.
- [13] ABB eStorage Max. <https://search.abb.com/library/Download.aspx?DocumentID=1VPD110001A0635&LanguageCode=en&DocumentPartId&Action=Launch> (accessed 2025).
- [14] D. Bazargan, *Hardware-in-loop simulation of battery storage systems for power system applications*. University of Manitoba (Canada), 2012.
- [15] S. E. NEB, "Overview of the pem silyzer family," 2020.
- [16] D. Wei, H. Li, Y. Ren, X. Yao, L. Wang, and K. Jin, "Modeling of hydrogen production system for photovoltaic power generation and capacity optimization of energy storage system," *Frontiers in Energy Research*, vol. 10, p. 1004277, 2022.